THE JOURNAL OF PHYSICAL CHEMISTRY B

ARTICLE

pubs.acs.org/JPCB

Volumetric Properties and Spectroscopic Studies of Pyridine or Nicotine Solutions in Liquid Polyethylene Glycols

Zoran P. Visak,*[,†] Laura M. Ilharco,[‡,§] Ana Rosa Garcia,[‡,§,∥] Vesna Najdanovic-Visak,[⊥] João M. N. A. Fareleira,[†] Fernando J. P. Caetano,[†,#] Mirjana L. Kijevcanin,[▽] and Slobodan P. Serbanovic[▽]

[†]Centro de Química Estrutural, [‡]Centro de Química-Física Molecular, and [§]IN—Institute of Nanoscience and Nanotechnology, Instituto Superior Técnico, Av. Rovisco Pais 1, 1049-001 Lisboa, Portugal

[∥]Departamento de Química e Farmácia, FCT, Universidade do Algarve, Campus de Gambelas, 8005-139 Faro, Portugal

[⊥]REQUIMTE, Departamento de Química, Faculdade de Ciências e Tecnologia, Universidade Nova de Lisboa, Quinta da Torre, 2829-516 Caparica, Portugal

[#]Departamento de Ciências e Tecnologia, Universidade Aberta, Rua da Escola Politécnica 147, 1269-001 Lisboa, Portugal

[▽]Faculty of Technology and Metallurgy, University of Belgrade, Karnegijeva 4, 11120 Belgrade, Serbia

Supporting Information

ABSTRACT: Densities and molar excess volumes of the solutions of pyridine or nicotine in liquid polyethylene glycol, PEG200 and PEG400, have been determined at several temperatures. The experimental molar excess volumes are negative, thus indicating strong attractive interactions between the components, as could be expected considering their highly polar nature and good hydrogen bond abilities. For the pyridine systems, this negativity is slightly increased as the temperature rises, while the opposite tendency is observed for the nicotine mixtures. When pyridine and nicotine solutions are compared, the former—particularly those with PEG400—exhibit substantially more negative molar excess volumes than the latter. The effect of the polymer chain length on the results for the nicotine solutions is almost negligible. However, this is not the case when pyridine is one of the components: a longer chain induced considerably higher compression on mixing. The Fourier-transform infrared analysis allowed interpretation of the negative experimental molar excess volumes in terms of specific inter- and intramolecular interactions.

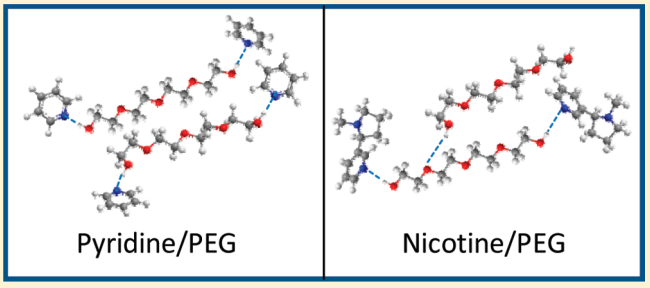

INTRODUCTION

Pyridine and nicotine are toxic chemical substances important from practical (economical), as well as fundamental, points of view. Pyridine is commonly used in organic synthesis; it is considered to be a versatile solvent and a fundamental building block and reagent.[1] Nicotine is (unfortunately) worldwide known as a major tobacco constituent, but plays an ever-growing role in pharmacology—as a potential drug against some neurodegenerative diseases.[2] These molecules have quite interesting features that allow a variety of interactions, as they possess lone (localized) electron pair(s) in nitrogen atoms, aromatic rings with their π-electron system, high polarity,[3,4] and hydrogen bond basicity (nucleophilicity),[5] nicotine being particularly disposed to (single or double) protonation.[6] Furthermore, the nicotine molecule has two different rings—one aromatic (pyridine) and one aliphatic (pyrrolidine). These show diverse rotation ability[7] and appear in different, nonplanar, spatial conformations, both in the gas phase and in (water) solutions.[7−9]

Polyethylene glycol (PEG) is a biodegradable and nontoxic, practically eatable, polymer, as can be concluded from its environmental characteristics and toxicological studies.[10] Its monomer and liquid forms are good, highly polar solvents.[11,12] Being both good proton donors and proton acceptors,[13] they have fine hydrogen bond formation ability. Hence, they are used as solvents for various homogeneously catalyzed reactions with supercritical CO_2[10,14] or in imide derivative synthesis.[15]

Our solubility tests showed that pyridine and nicotine are completely miscible in liquid PEG with average molecular weights of 200 and 400 (PEG200 and PEG400, respectively). Thus, liquid PEGs are good, ambient friendly solvents for these toxic compounds. The thermophysical properties of these solutions are very useful in any future design or development of potential chemical reactions or chemical engineering processes (extraction and/or separation) that involve these solutions. To the best of our knowledge, there is, so far, an extensive lack of thermophysical property data on these systems. In particular, no

Received: March 15, 2011
Revised: May 19, 2011
Published: May 23, 2011

volumes of mixing could be found in the literature. From the fundamental point of view, the present systems are also very appealing due to the aforementioned features of their constituents.

Therefore, in this study we have measured densities of the pyridine or nicotine + PEG200 or PEG400 solutions at ambient pressure and in the range from 288.15 to 333.15 K. On the basis of these data, molar excess volumes were calculated. Further on, Fourier-transform infrared (FTIR) spectroscopy studies of all the pure compounds and mixtures were performed to obtain insight into major inter- and intramolecular interactions in the studied mixtures.

All the results, including the spectroscopic studies, indicate the presence of strong attractive interactions in the solutions—hydrogen bonds and, particularly, dipole−dipole interactions: Keesom and dispersive forces. The obtained spectra are in agreement with the trends of the measured V^E values. At the same time they concur with the interesting claims[16] that extending the length of the polymer chain induces and supports the helical shape formation of PEG.

Although the infrared and Raman spectra of the pyridine and pyrrolidine rings have been thoroughly analyzed,[17−21] the same is not true for the complete vibrational spectrum of nicotine; only partial analyses could be found in the literature,[22,23] and some bands have been used mainly for quantitative purposes.[21] To the best of our knowledge, we present the first complete analysis of the nicotine vibrational spectrum.

The novelty of the present work consists in a twofold approach to the pyridine/liquid polyethylene glycol and nicotine/liquid polyethylene glycol systems, complementing the volumetric properties with spectroscopic studies that allowed interpretation of the thermodynamic data.

EXPERIMENTAL SECTION

Chemicals and Preparation of Solutions. All the chemicals were purchased from Sigma-Aldrich, with a stated minimum purity of 99 wt % for nicotine, PEG200, and PEG400 and 99.5 wt % for pyridine. For PEG200 and PEG400 the molar mass varied between 190 and 210 kg kmol $^{-1}$ and between 380 and 420 kg kmol^{-1}, respectively. The chemicals were dried for 48 h using 3 Å molecular sieves and kept under a nitrogen atmosphere. Pyridine and particularly nicotine were protected from light. However, both PEGs were additionally treated under vacuum (0.1 Pa) for 48 h, at about 60 °C, immediately prior to the measurements. Coulometric Karl Fischer titration revealed the following contents of water after drying: pyridine, 50 ppm; nicotine, 80 ppm; PEG 200, 300 ppm; PEG400, 450 ppm. The solutions were prepared gravimetrically using a high-precision Mettler analytical semimicrobalance (model AT201) which has a stated repeatability of $\pm 2 \times 10^{-5}$ (mass fraction) in a typical, nondiluted region of measurements.

Density Measurements. Density was measured in the temperature range of 288.15−333.15 K using a DMA5000 Anton-Paar vibrating tube densimeter.

Spectroscopic Studies. The molecular structures of PEG200 and PEG400 were analyzed by FTIR in transmission mode using a Mattson RS1 FTIR spectrometer in the 4000−400 cm^{-1} range (wide-band MCT detector) at 2 cm^{-1} resolution. The samples were prepared by depositing a drop of the polymer between two KBr windows. The spectra were the result of 100 added scans for each sample, ratioed against the same number of scans for the background (the clean KBr windows). Their mixtures with pyridine and nicotine, with compositions corresponding to the minimum V^E in each case, were also analyzed. All the spectroscopic studies were performed at 298.15 K.

Table 1. Densities of the Pure Studied Substances at Several Temperatures and Their Comparison with Values from the Literature

		ρ/kg m^{-3}	
compound	T/K	this work	literature
PEG200	298.15	1120.69	1120.98[24]
	303.15	1116.70	1117.01[24]
PEG400	298.15	1122.33	1122.49[24]
			1122.30[25]
			1121.80[26]
			1121.62[26]
	303.15	1118.22	1118.31[24]
			1118.00[26]
	308.15	1114.13	1114.20[26]
	313.15	1110.04	1109.70[26]
			1110.20[27]
	318.15	1105.96	1105.70[26]
			1106.40[27]
	323.15	1101.89	1101.70[26]
			1102.00[27]
pyridine	293.15	983.18	983.19[28]
	298.15	978.14	978.24[28]
	303.15	973.09	973.19[28]
nicotine	298.15	1004.98	1006.77[29]

RESULTS AND DISCUSSION

Molar Excess Volumes. Measured densities of the pure compounds and their comparison with values from the literature[24−29] are given in Table 1. The densities and molar excess volumes of the studied mixtures are given in Table S1 of the Supporting Information. Molar excess volumes were calculated using the equation

$$V^E = \frac{M}{\rho} - \sum x_i \frac{M_i}{\rho_i} \quad (1)$$

in which M and ρ represent the mixture molar mass and its density, respectively, while x_i, M_i, and ρ_i stand for the pure component mole fraction, molar mass, and density, respectively.

Calculated molar excess volumes are shown in Figures 1−4. It can be seen that they are negative for all the studied systems. Molar excess volumes of the pyridine systems become more negative as the temperature increases; this tendency is reversed for the studied nicotine mixtures. This behavior may be caused by the different values of the isobaric thermal expansion coefficients, α_p, of the pure components. In fact, this coefficient for pyridine is about 50% higher than the values of α_p for PEG200 and PEG400, which are practically equal. However, in the case of nicotine, α_p is much lower—only about 10% higher than the expansion coefficient for the PEGs. Moreover, the critical temperature of nicotine is calculated to be 742.9 K. (To the best of our knowledge, no literature data on the critical temperature of nicotine exist. Thus, it was calculated using nicotine's normal boiling point (T_{bn} = 520 K)

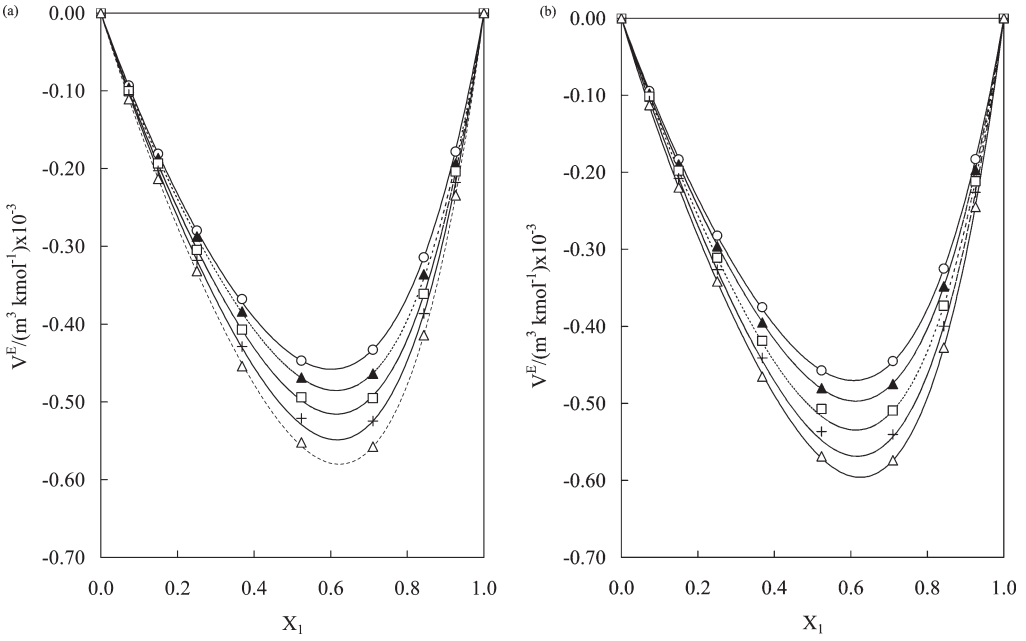

Figure 1. Molar excess volumes at ambient pressure of the pyridine (1) + PEG200 (2) solutions: (a) △, 288.15 K; +, 298.15 K; □, 308.15 K; ▲, 318.15 K; ○, 328.15 K; (b) △, 293.15 K; +, 303.15 K; □, 313.15 K; ▲, 323.15 K; ○, 333.15 K. x_1 stands for the molar fraction of pyridine. The lines represent RK polynomial fittings of the experimental data.

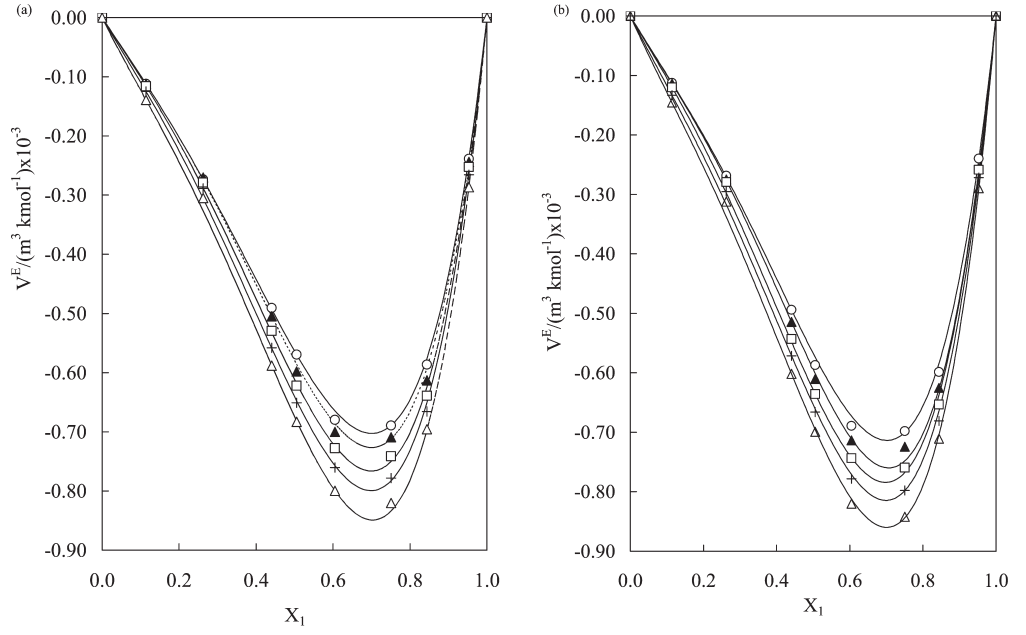

Figure 2. Molar excess volumes at ambient pressure of the pyridine (1) + PEG400 (2) solutions: (a) △, 288.15 K; +, 298.15 K; □, 308.15 K; ▲, 318.15 K; ○, 328.15 K; (b) △, 293.15 K; +, 303.15 K; □, 313.15 K; ▲, 323.15 K; ○, 333.15 K. x_1 stands for the molar fraction of pyridine. The lines represent RK polynomial fittings of the experimental data.

and the widely accepted ratio T_c/T_{bn} = 0.7 for the hydrogen-bonding substances.) This calculated value is significantly higher than that of pyridine (620.1 K),[30] and it is thus closer to the critical temperatures of the liquid PEG200 and PEG400 (726.6 and 839.4 K, respectively).[31] Consequently, a temperature increase leads to a more significant relative expansion of pure pyridine than of the liquid polymer; thus, according to eq 1, it contributes to more negative molar excess volumes than in the nicotine systems. Additionally, the temperature increase diminishes the strength of the dominant hydrogen bonds, the prevailing effect of which is the relaxation of the three-dimensional structure of the solutions with pyridine. Thus, even though the hydrogen bonds are weaker, the V^E values are more negative as the temperature rises. However, in the nicotine solutions, hydrogen bonds are much weaker and more dominant dispersion interactions decrease substantially as the temperature rises, while the conformational

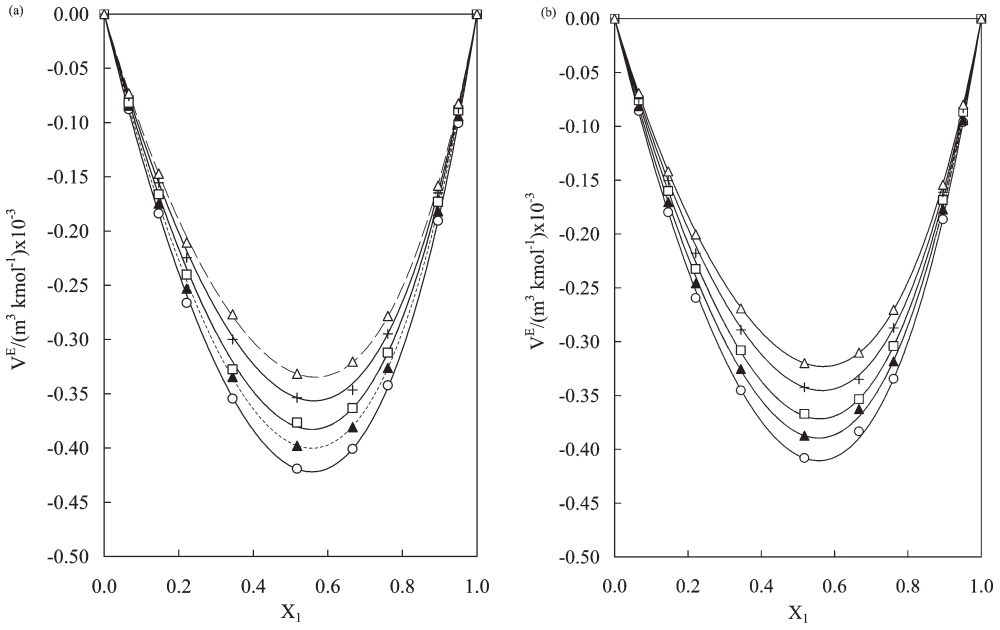

Figure 3. Molar excess volumes at ambient pressure of the nicotine (1) + PEG200 (2) solutions: (a) △, 288.15 K; +, 298.15 K; □, 308.15 K; ▲, 318.15 K; ○, 328.15 K; (b) △, 293.15 K; +, 303.15 K; □, 313.15 K; ▲, 323.15 K; ○, 333.15 K. x_1 stands for the molar fraction of nicotine. The lines represent RK polynomial fittings of the experimental data.

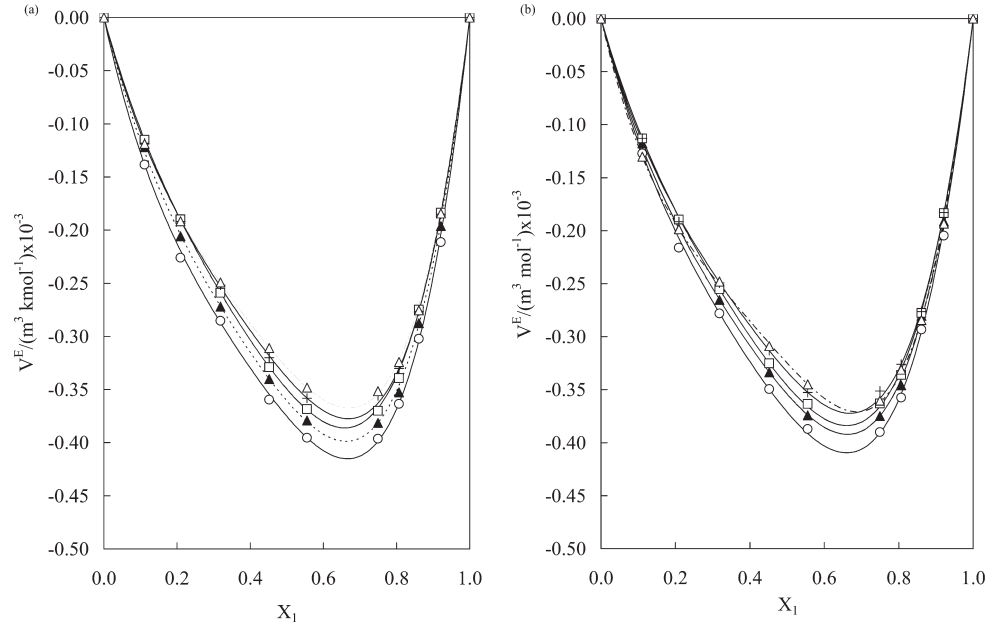

Figure 4. Molar excess volumes at ambient pressure of the nicotine (1) + PEG400 (2) solutions: (a) △, 288.15 K; +, 298.15 K; □, 308.15 K; ▲, 318.15 K; ○, 328.15 K; (b) △, 293.15 K; +, 303.15 K; □, 313.15 K; ▲, 323.15 K; ○, 333.15 K. x_1 stands for the molar fraction of nicotine. The lines represent RK polynomial fittings of the experimental data.

rearrangements—as shown in the related spectra—do not exist (see below). Consequently, the rise in temperature provokes less negative V^E values.

The reported experimental molar excess volumes were fitted using a Redlich−Kister (RK) equation:

$$V^E = x_1 x_2 \sum_{k=0}^{k=2} A_k (x_1 - x_2)^k \qquad (2)$$

The A_k coefficients for each isotherm are presented in Table 2, along with the standard deviations σ. Table 2 shows a very good fitting of the experimental V^E values using only three RK parameters.

The present results point toward the existence of strong attractive interactions between the components. These were expected since all the constituents have very good hydrogen bond abilities: nicotine and pyridine are both excellent hydrogen bond acceptors (they have high and similar hydrogen bond

dx.doi.org/10.1021/jp202464h |J. Phys. Chem. B 2011, 115, 8481–8492

Table 2. Coefficients of the Redlich−Kister Expansion (eq 2) Used for the Fitting of the Experimental Molar Excess Volume Data

T/K	A_0	A_1	A_2	σ^a
		Pyridine (1) + PEG200 (2)		
288.15	−1.75858	−0.69055	−0.30014	0.00203
293.15	−1.79707	−0.74834	−0.31218	0.00139
298.15	−1.84356	−0.80974	−0.38116	0.00264
303.15	−1.88928	−0.82888	−0.36716	0.00093
308.15	−1.95589	−0.87765	−0.384034	0.00247
313.15	−2.02856	−0.91842	−0.34422	0.00455
318.15	−2.07569	−0.96382	−0.38770	0.00374
323.15	−2.14978	−1.00803	−0.38147	0.00576
328.15	−2.18178	−1.05607	−0.47300	0.00273
333.15	−2.23752	−1.09370	−0.51541	0.00213
		Pyridine (1) + PEG400 (2)		
288.15	−2.25414	−2.2729	−1.09997	0.01035
293.15	−2.26958	−2.36868	−1.13041	0.01172
298.15	−2.31807	−2.41186	−1.10363	0.01260
303.15	−2.37755	−2.59479	−1.26349	0.01139
308.15	−2.44621	−2.55291	−1.13098	0.00941
313.15	−2.51496	−2.5946	−1.13472	0.01197
318.15	−2.56312	−2.63434	−1.18529	0.01089
323.15	−2.61461	−2.65238	−1.26742	0.01332
328.15	−2.69746	−2.79853	−1.41366	0.01169
333.15	−2.75203	−2.78964	−1.41878	0.01285
		Nicotine (1) + PEG200 (2)		
288.15	−1.66659	−0.36716	−0.12657	0.00324
293.15	−1.62256	−0.34862	−0.12649	0.00380
298.15	−1.58108	−0.34494	−0.12041	0.00304
303.15	−1.53922	−0.33294	−0.11960	0.00414
308.15	−1.51218	−0.33198	−0.11081	0.03683
313.15	−1.46636	−0.33693	−0.10786	0.00289
318.15	−1.40468	−0.33252	−0.15036	0.00371
323.15	−1.35917	−0.33457	−0.16487	0.00339
328.15	−1.31686	−0.32306	−0.17469	0.00237
333.15	−1.26990	−0.32028	−0.18326	0.00115
		Nicotine (1) + PEG400 (2)		
288.15	−1.50110	−0.81015	−0.87434	0.00479
293.15	−1.4841	−0.82911	−0.73836	0.00538
298.15	−1.44315	−0.80002	−0.75853	0.00367
303.15	−1.41728	−0.80095	−0.72152	0.00339
308.15	−1.39915	−0.80005	−0.63906	0.00309
313.15	−1.38512	−0.81040	−0.64411	0.00286
318.15	−1.35395	−0.78573	−0.74583	0.00307
323.15	−1.33216	−0.78109	−0.74328	0.00387
328.15	−1.31765	−0.74880	−0.77560	0.00272
333.15	−1.30054	−0.75806	−1.00306	0.00222

[a] Standard deviation calculated by $\sigma = [[\Sigma_n(V^E_{calcd} - V^E_{exptl})_n^2]/(n-m)]^{1/2}$, where n is the number of experimental points and m stands for the number of A_k coefficients.

basicities,[5] and the molecule of nicotine has two protonation sites[6]). PEGs are both good proton donors and good proton acceptors (they possess hydrogen bond acidity as well as basicity).[13] Moreover, all these compounds have a distinguished polar nature: the pyridine dipole moment[3] is 2.22 D, whereas that of nicotine[4] is 1.81 D. PEG 200 and PEG400 have particularly high polarities:[11,12] 3.06−3.94 and 3.70−4.96 D at room temperature, respectively. Nevertheless, when the results at constant temperature (298.15 K) are compared, the figures reveal the following: (i) for the same PEG, pyridine solutions

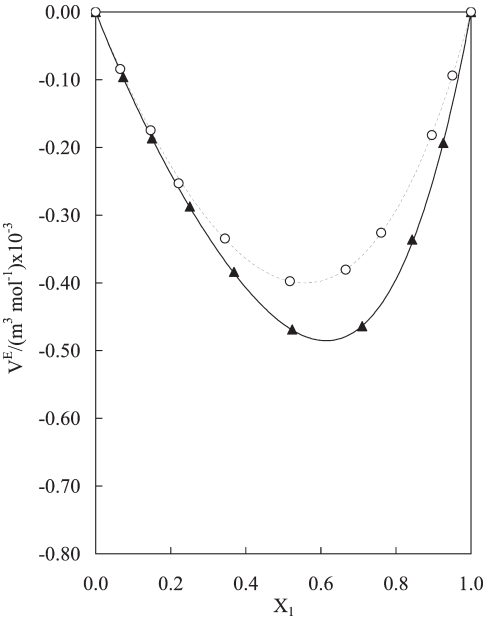

Figure 5. Comparison at 298.15 K of the molar excess volumes of the pyridine and nicotine solutions with PEG200: ○, nicotine + PEG200; ▲, pyridine + PEG200. The lines represent RK polynomial fittings of the experimental data.

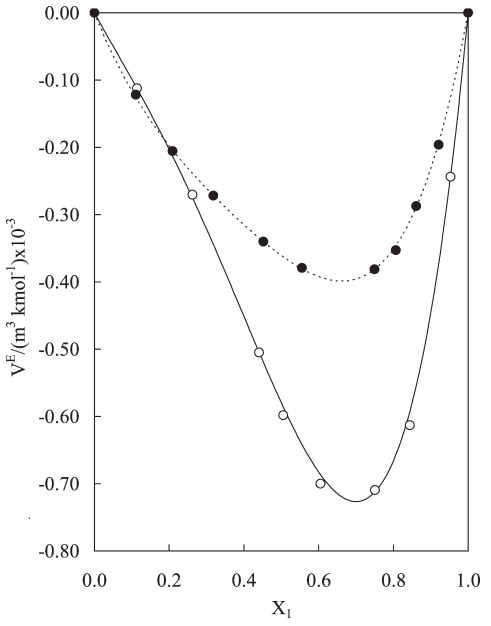

Figure 6. Comparison at 298.15 K of the molar excess volumes of the pyridine and nicotine solutions with PEG400: ●, nicotine + PEG400; ○, pyridine + PEG400. The lines represent RK polynomial fittings of the experimental data.

dx.doi.org/10.1021/jp202464h |J. Phys. Chem. B 2011, 115, 8481–8492

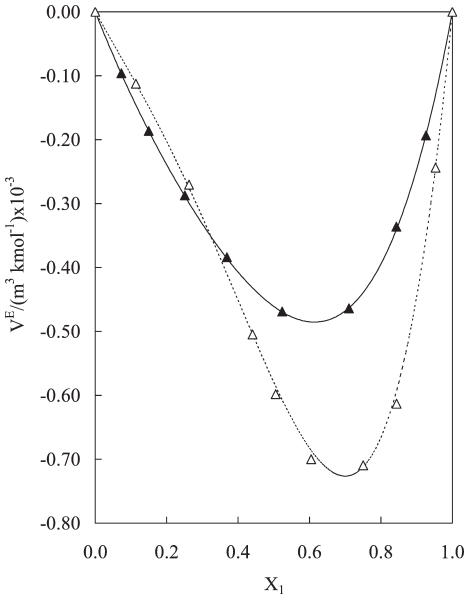

Figure 7. Comparison at 298.15 K of the molar excess volumes of the pyridine solutions with PEG200 and PEG400: ▲, pyridine + PEG200; △, pyridine + PEG400. The lines represent RK polynomial fittings of the experimental data.

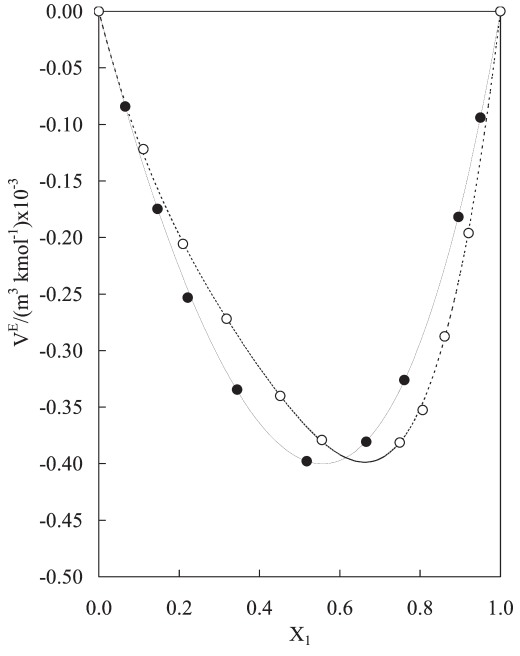

Figure 8. Comparison at 298.15 K of the molar excess volumes of the nicotine solutions with PEG200 and PEG400: ●, nicotine + PEG200; ○, nicotine + PEG400. The lines represent RK polynomial fittings of the experimental data.

show significantly more negative values of V^E than those of nicotine (Figures 5 and 6); (ii) when the effect of the PEG chain is considered, the pyridine solutions with PEG400 exhibit larger negative V^E values than those with PEG200 (Figure 7), although the hydrogen bond acidity of the neat PEG200 is higher than that of PEG400;[13] (iii) for the studied nicotine solutions, the polymer chain has practically no effect on the molar excess volumes (Figure 8).

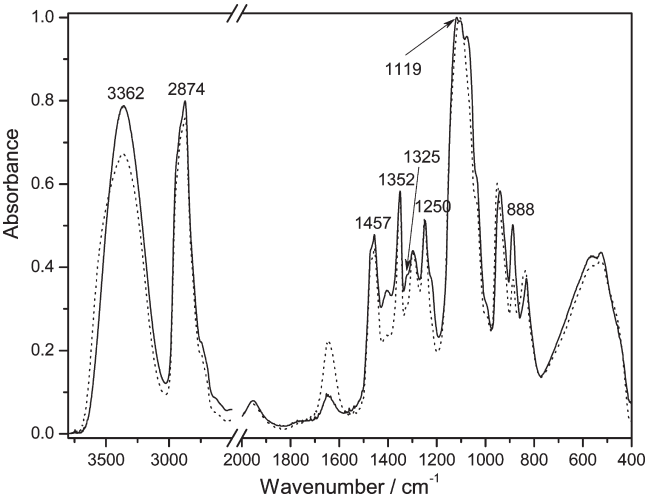

Figure 9. Infrared spectra of PEG200 (solid) and PEG400 (dotted) normalized to the maximum absorption.

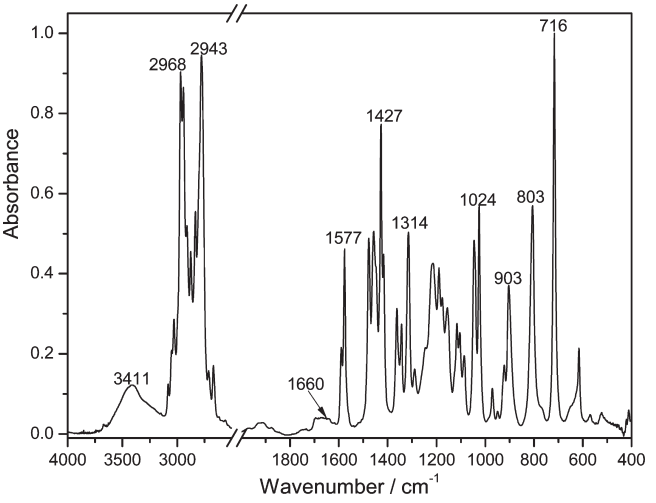

Figure 10. Infrared spectrum of pure nicotine.

With respect to the first comparison outcome, it is a priori reasonable to suspect that the difference in size between pyridine and nicotine molecules obviously contributes to the more negative values of molar excess volumes of the pyridine systems. On the other hand, the nonplanar conformations of the two rings of nicotine[7−9] do not seem to be very compatible with large PEG molecules, impeding dense packing. Finally, pyridine is more polar than nicotine. However, observations ii and iii cannot be explained in a straightforward manner, only taking into account the aforementioned properties of the pure compounds. Thus, the FTIR spectra of the pure components and of the mixtures corresponding to the minimum excess volumes were analyzed, with the aim of gaining better insight into the molecular interactions.

FTIR Analysis. *Pure Components.* The influence of the chain length on the molecular structure and conformations of PEG was examined by comparing their FTIR spectra (Figure 9). They were assigned taking into account previously published analysis.[32−34]

In both polymers, the position of the OH stretching band (maximum absorption at ∼3360 cm^{-1}) and its broad profile indicate that the terminal hydroxyl groups are involved in a

dx.doi.org/10.1021/jp202464h |*J. Phys. Chem. B* 2011, 115, 8481–8492

Table 3. Assignments of the Infrared Bands of Pure Nicotine

wavenumber/cm^{-1}		band assignment[22,23]
3411	w, br	ν(OH) (residual water)
3083	w	ν(CH) (Pyrr ring)
3051	w, sh	ν(CH) (Py ring)
3030	m	ν(CH) (Py ring)
2968	vs	ν_{as}(CH$_3$) (methyl-Pyrr)
2943	vs	ν_{as}(CH$_2$) (Pyrr)
2911	m, "sh"	ν_{as}(CH$_2$) (Pyrr)
2876	m	ν_s(CH$_2$) (Pyrr)
2834	s	ν_s(CH$_3$) (methyl-Pyrr)
2779	vs	combination band
2712	w	
2669	w	
1660	w, vbr	δ(HOH) (residual water)
1590	w	ν(C$_\alpha$−C$_\beta$) (Py ring)
1577	m	ν(C$_\beta$−C$_\gamma$) (Py ring)
1477	m	δ_{as}(CH$_2$) (back) (Pyrr)
1457	m	δ_s(CH$_2$) (back) (Pyrr)
1449	m, sh	δ_sCH$_2$ (for) (Pyrr)
1427	s	δ_{as}(CH$_3$) (methyl-Pyrr)
1416	m, sh	δ_s(CH$_2$) (for) (Pyrr)
1362	m	ω_{as}(CH$_2$) (for) (Pyrr)
1343	m	ω_{as}(CH$_2$) (back) (Pyrr)
1314	m	ω(C−N−C) (methyl-Pyrr)
1289	w	ω_s(CH$_2$) (for) (Pyrr)
1245	w, sh	
1215	m	τ_s(CH$_2$) (for)
1190	m	τ_s(CH$_2$) (back)
1176	m	τ_{as}(CH$_2$) (for)
1155	m	C$_\beta$HC$_\gamma$H def (Py ring)
1116	m	ν_{as}(C−N−C)
1104	m	
1087	w	C$_\gamma$H def, C$_\alpha$H and C$_\beta$H sym def (Py ring)
1046	s	C$_\alpha$H and C$_\beta$H asym def, CCC and CNC def (Py ring)
1025	s	ring breathing (Py and Pyrr rings)
971	w	ω_{as}(C$_\alpha$H, C$_\beta$H) (Py ring)
949	vw	
922	w	ρ(CH$_3$)
903	m	ρ_{as}(CH$_2$)
806	s	ρ_s(CH$_2$)
716	vs	ω_s(CH) (Py ring)
616	w	δ(C−N−C) (in-plane)

variety of strong hydrogen bonds (HBs). This agrees with the well-established fact that these groups may act as both HB donors and HB acceptors.[13] Although the maximum of this band does not shift, the full width at half-maximum increases from 350 cm^{-1} in PEG200 to 410 cm^{-1} in PEG400, with a clear broadening to the higher wavenumber region. This suggests the coexistence of some weaker H bond interactions involving those groups of PEG400, probably within the same polymer chain. The ν(OH) modes of residual water could also contribute to this band. However, in PEG200 this contribution is irrelevant since the very weak water deformation mode (at 1640 cm^{-1}) shows that the amount of water present is negligible. For PEG400 this band is slightly stronger, which is not surprising because there is a much higher number of ether groups with which water molecules may interact, and an exhaustive drying becomes more difficult.

The profiles of the CH$_2$ stretching and scissors bands (with maxima at 2874 and 1457 cm^{-1}, respectively) do not change with the chain length, but evidence the presence of overlapping components. The stretching band may contain unresolved symmetric and asymmetric modes; however, the components in the scissors band may only be explained by the presence of different chain conformations (*trans* and *gauche*).[34] The CH$_2$ groups are also responsible for bands near 1352 cm^{-1} (wagging), 1250 cm^{-1} (twisting), 940 cm^{-1} (rocking of *gauche* isomers), and 888 cm^{-1} (rocking of *trans* conformers). These bands occur at the same position for both polymers, except for the ρ(CH$_2$) mode (*gauche*) that shifts from 940 cm^{-1} in PEG200 to 952 cm^{-1} in PEG400. This mode appears to be more sensitive to the bond angles at the *gauche* conformations, which may be different for the two polymer chains. The fact that the ρ(CH$_2$) mode (*trans*) is relatively stronger for PEG200 suggests a different conformational distribution for the two chains, with predominance of *trans* conformers for the shorter one. Another indication is supplied by the CH$_2$ wagging mode of *trans* conformers, which appears as a shoulder (at 1325 cm^{-1}),[33] with a higher relative intensity with respect to the corresponding *gauche* mode (at 1352 cm^{-1}) for PEG200.

In the skeletal band region (1200−950 cm^{-1}), the C−O−C, C−OH, and C−C stretching modes are partially overlapped and were recovered by decomposition in a sum of Voigt components (convolution of Gaussian and Lorentzian profiles) by a nonlinear least-squares fitting method, as shown in Figure S1 of the Supporting Information). The different band profiles for the two polymer chains result mainly from changes in the components' relative intensities, as summarized in Table S2 (Supporting Information).

The influence of the chain length is evident when comparing the relative intensities of the components related to the terminal groups: ν(C−C) (at 993 or 994 cm^{-1}), ν(C−OH) (at 1064 or 1061 cm^{-1}), and δ(CH$_2$) (at 1143 or 1149 cm^{-1}), which are more relevant for the shorter chain of PEG200. On the other hand, the presence of two ν(C−O−C) modes confirms that different chain conformations coexist. The component at lower frequencies (1100 or 1089 cm^{-1}) is assigned to the *trans* conformer and the other one (1124 or 1123 cm^{-1}) to conformers with *gauche* rotations. The last row of Table S2 (Supporting Information) confirms quantitatively that the *trans* conformers predominate for PEG200 (the relative area of the ν(C−O−C) mode for *trans* conformers is 65%), whereas for PEG400 the two types of conformers have approximately the same population (the relative area of the ν(C−O−C) mode for *trans* conformers is 49%). This different conformational distribution may also be responsible for the smaller relative area of the ν(C−C) (chain) band for PEG400, as the C−C stretching may be more hindered in *gauche* chains. These observations are in good agreement with the previous results that correlate a higher average molecular weight of PEG with a more helical structure.[16] Overall, there are only small shifts in the retrieved components when comparing the two polymers, with the exception of the ν(C−O−C) (T) mode, which appears 11 cm^{-1} to lower wavenumbers for PEG400. This is consistent with a higher involvement of the ether oxygens in hydrogen bonds, either intermolecular (with OH groups of a different chain or of residual

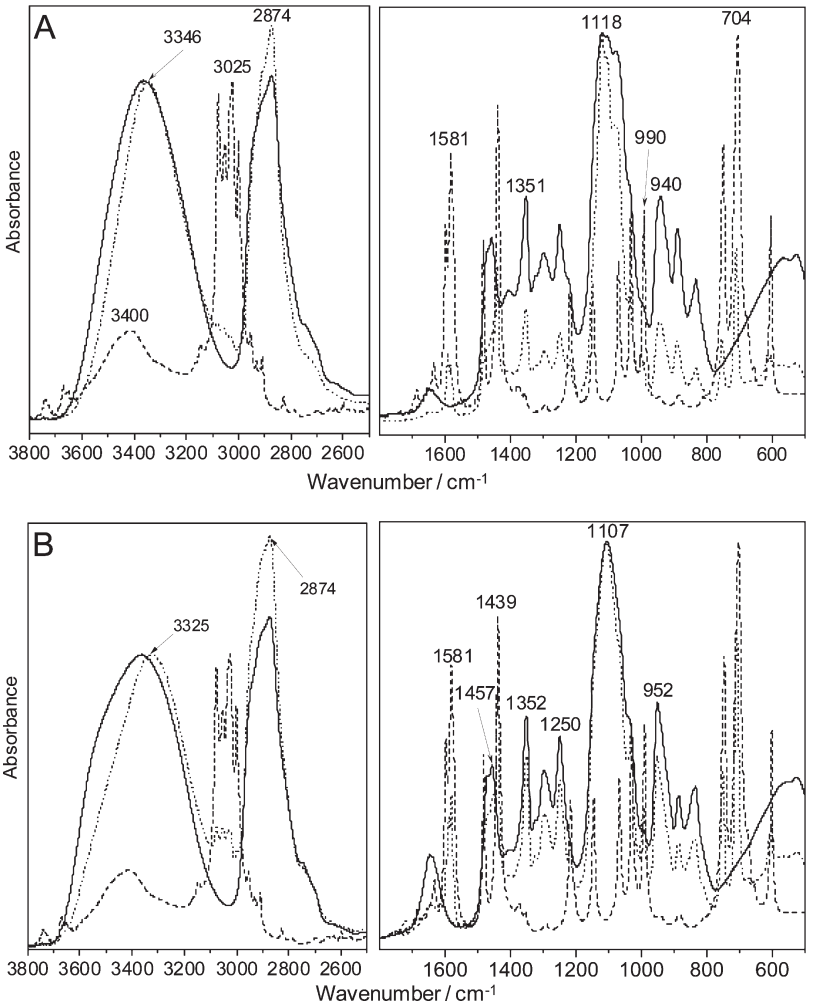

Figure 11. Infrared spectra of (A) pure PEG200 (solid), pure pyridine (dashed), and the mixture pyridine + PEG200 with x_{PEG200} = 0.47628 (dotted) and (B) pure PEG400 (solid), pure pyridine (dashed), and the mixture pyridine + PEG400 with x_{PEG400} = 0.2495 (dotted). The spectra were normalized to the ν(OH) and ν(C−O−C) bands of PEG in the high- and low-wavenumber regions, respectively.

water) or intramolecular (with the terminal OH groups of the same chain). The latter could account for the aforementioned weaker H bonds suggested by the profile of the ν(OH) band of PEG400.

The infrared spectrum of pure nicotine obtained in the present work is shown in Figure 10. The small bands centered at ∼3411 and ∼1660 cm^{-1} indicate that there is some residual water even in nicotine dried over molecular sieves. The proposed band assignments for pure nicotine are summarized in Table 3.

The infrared spectrum of pure pyridine has been thoroughly analyzed in the literature[17−20] and is only shown for comparison with the spectra of the mixtures (Figure 11).

Pyridine + PEG200/400 Solutions. The infrared spectra of pyridine + PEG200/PEG400 mixtures with the compositions corresponding to the minimum excess volume at 298.15 K are compared with those of the pure components in Figure 11. From this comparison, information on the established interactions may be inferred.

In the pyridine + PEG200 mixture (Figure 11A), the ν(OH) band becomes much narrower than in the pure polymer and shifts noticeably to a lower wavenumber (from 3362 to 3346 cm^{-1}). These effects are even more pronounced in the pyridine + PEG400 mixture (see Figure 11B), where the shift is from 3362 to 3325 cm^{-1}. There are a majority of hydrogen bonds between the hydroxyl groups of PEG and pyridine which

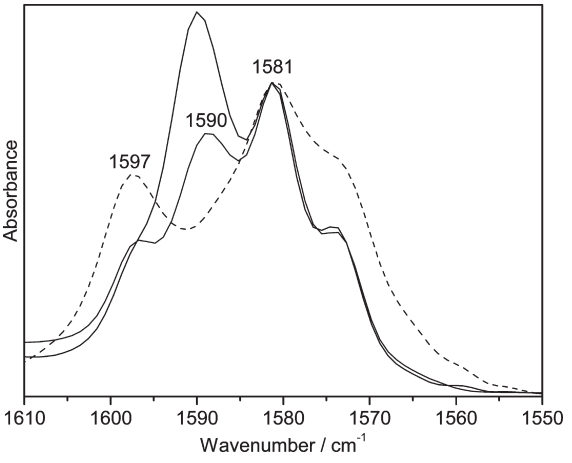

Figure 12. Spectral region between 1610 and 1550 cm^{-1} for pure pyridine (dashed) and pyridine + PEG200 (solid black) and pyridine + PEG400 (solid gray) mixtures normalized to the band at 1581 cm^{-1}.

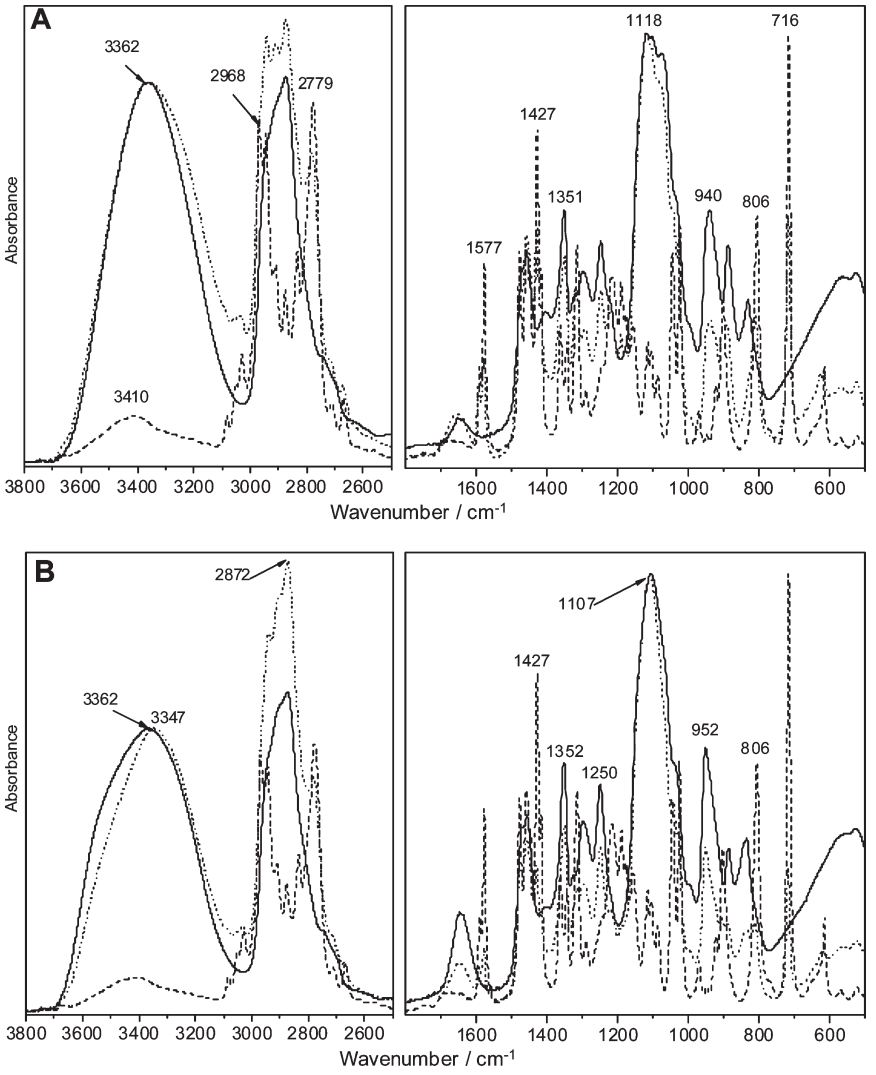

Figure 13. Infrared spectra of (A) pure PEG200 (solid), pure nicotine (dashed), and the mixture nicotine + PEG200 with x_{PEG200} = 0.45560 (dotted) and (B) pure PEG400 (solid), pure nicotine (dashed), and the mixture nicotine + PEG400 with x_{PEG400} = 0.43256 (dotted). The spectra were normalized to the ν(OH) and ν(C−O−C) bands of PEG in the high- and low-wavenumber regions, respectively.

are stronger and more uniform than those among PEG molecules themselves and between pyridine and residual water (since the ν(OH) mode in the pyridine spectrum appears at ∼3400 cm^{-1}). Both the nitrogen atom and the aromatic system of pyridine act as good hydrogen bond acceptors. Moreover, intermolecular hydrogen bonds are stronger in the pyridine + PEG400 solution, which may contribute to explaining the comparative results in Figure 7.

The frequencies of the CH_2 stretching and rocking bands of each PEG chain do not change when PEG is mixed with pyridine. Thus, there are no angular modifications in the *gauche* conformers due to the presence of this solute.

In the region corresponding to the polymer skeletal modes (1200−950 cm^{-1}), the spectral deconvolution was also made for pure pyridine and for the pyridine + PEG200/PEG400 solutions; see Figure S2 in the Supporting Information. Six Voigt components were retrieved for pure pyridine, as shown in Figure S2A: at 991 cm^{-1} (ring breathing), 1030 cm^{-1} (C_αH and C_βH asymmetric deformation, CCC and CNC deformation), 1068 cm^{-1} (C_αH and C_βH asymmetric deformation, CCC bend), and 1147 cm^{-1} ($C_\beta HC_\gamma H$ deformation), plus the very weak ones at 980 cm^{-1} (C_αH and C_βH asymmetric wagging) and at 1089 cm^{-1} (C_γH bend, C_αH and C_βH symmetric deformation).

The best fittings obtained for the pyridine + PEG200/PEG400 mixtures are shown inFigure S2B,C, and the fitting results are summarized in Table S3 (Supporting Information). The relative intensities (% area) are included for comparison within each spectrum, as some of the components retrieved are assigned to overlapping bands of the polymer and of pyridine, rendering difficult a comparison between the spectra.

The weaker component of the polymer (ν(C−C) (terminal), at 993 or 994 cm^{-1}) is not relevant in the spectra of the mixtures. The same is true for the very weak C_αH and C_βH asymmetric wag of pyridine at 980 cm^{-1}.

The ring breathing of pyridine (991 cm^{-1}) appears as a doublet in both mixtures: at 989/999 cm^{-1} in pyridine + PEG200 and at 990/998 cm^{-1} in pyridine + PEG400. This may be explained by a deformation of the pyridine molecule resulting from the interactions with the polymer—not only the very strong and directional hydrogen bonds revealed by the

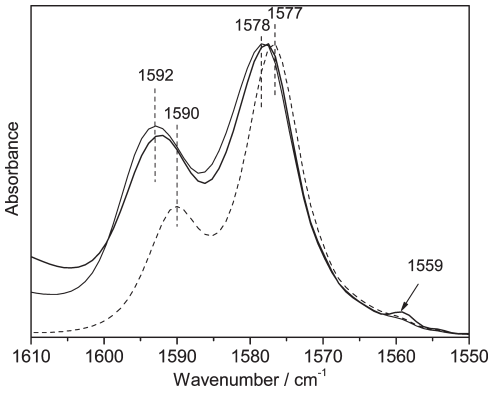

Figure 14. Spectral region between 1610 and 1550 cm^{-1} for pure nicotine (dashed) and nicotine + PEG200 (solid black) and nicotine + PEG400 (solid gray) mixtures normalized to the band at ~1577 cm^{-1}.

ν(OH) band of PEG, but also strong dispersion and Keesom interactions that are expected considering the high polarizabilities and dipole moments of the components, particularly for the pair pyridine/PEG400. Furthermore, these interactions contribute to the negative molar excess volumes of the pyridine + PEG200/PEG400 solutions.

The components recovered at ~1030, ~1069, and ~1140 cm^{-1} correspond to the overlapping modes of pyridine and polymer, but the ν(C−O−C) modes of PEG and the $C_\gamma H$ deformation and $C_\alpha H$ and $C_\beta H$ symmetric deformation of pyridine are identified independently. In the pyridine + PEG200 mixture, the *trans* and *gauche* ν(C−O−C) frequencies do not change with respect to those of the pure polymer, which confirms that the pyridine/polymer-specific interactions are not related to the ether oxygen of the polymer. Nevertheless, the relative intensities of the two ν(C−O−C) modes become very similar, which means that the conformational distribution shifts toward the *gauche* in the presence of pyridine. The same tendency, but on a much larger scale, is observed for PEG400. In this case, the shift of ν(C−O−C) (T) to a higher wavenumber with respect to the pure polymer (from 1089 to 1097 cm^{-1}) concurs with the preferential involvement of pyridine, rather than the ether oxygen atoms of the polymer, in H bonds with the OH groups.

The symmetry reduction in the pyridine molecule due to the interactions with the polymer is also apparent from the changes observed in the doublet at 1597/1581 cm^{-1}, assigned to the $\nu(C_\alpha{-}C_\beta)/\nu(C_\beta{-}C_\gamma)$ modes (Figure 12). For pure pyridine, the relative intensity of the $\nu(C_\beta{-}C_\gamma)$ component (1581 cm^{-1}) is higher. In the pyridine + PEG200 mixture, where x_{Py} is ~0.6, the $\nu(C_\alpha{-}C_\beta)$ component becomes the strongest and shifts to 1590 cm^{-1}. In the mixture pyridine + PEG400, where x_{Py} is ~0.7, there is a fraction of pyridine molecules interacting with the polymer responsible for the same shift of the $\nu(C_\alpha{-}C_\beta)$ band, although keeping the relative intensity. The shoulder at 1597 cm^{-1} is assigned to the fraction of unaffected aromatic molecules.

The pyridine−PEG interactions suggested by the FTIR spectra may provide a complementary explanation for the shift to more negative values of the molar excess volumes with increasing temperature: since the dominant hydrogen bonds are highly directional and their intensity decreases slightly with temperature,[35] the three-dimensional arrangement may be relaxed and a somewhat more dense packing facilitated due to the flexibility of pyridine. Obviously, this effect, leading to a more negative V^E, would prevail over the decrease in attractive interactions with increasing temperature, which favors a less negative V^E.

Nicotine + PEG200/PEG400 Solutions. A similar approach was used to study the nicotine + PEG200/400 solutions. The infrared spectra of solutions with compositions corresponding approximately to the minimum excess volume were compared with those of the pure components (Figure 13).

For the nicotine + PEG200 mixture, the ν(OH) band is broader, but the maximum is only slightly shifted to lower wavenumbers (from 3362 cm^{-1} in pure PEG200 to 3357 cm^{-1}), suggesting that the hydroxyl groups are involved in a wider variety of hydrogen bonds, but the majority are similar in strength to those among PEG molecules when pure. However, for the nicotine + PEG400 solution, the band is narrower than for the pure polymer. Also, it is considerably shifted to lower wavenumbers (~15 cm^{-1}), indicating that PEG400 and nicotine interact by more similar hydrogen bonds, the weaker interactions between PEG chains (possibly the intramolecular ones) having been replaced by PEG−nicotine H bonds. However, the shifts in the ν(OH) band are much smaller than those observed for the corresponding mixtures with pyridine, thus pointing to much weaker hydrogen bonds.

The stretching modes of the PEG methylene groups overlap those of nicotine ($\nu_{as}(CH_2)$ at 2943 and 2911 cm^{-1}, $\nu_s(CH_2)$ at 2876 cm^{-1}, $\nu_{as}(CH_3)$ at 2968 cm^{-1}, and $\nu_s(CH_3)$ at 2834 cm^{-1}), but the spectra of the mixtures display unshifted shoulders that suggest little mutual influence. The same information is retrieved from the methyl and methylene deformation bands, positioned in the 1480−1416 cm^{-1} region.

The spectral deconvolution in the region corresponding to the skeletal modes of the polymers (1200−950 cm^{-1}) did not yield relevant results because there are a large number of nicotine bands in the same region essentially due to the pyrrolidine ring.

The possibility of deformations in the pyridine ring of nicotine due to interactions with the polymer was also analyzed in terms of the $\nu(C_\alpha{-}C_\beta)/\nu(C_\beta{-}C_\gamma)$ modes that appear as a doublet at 1590/1577 cm^{-1} in pure nicotine (Figure 14). This spectral region is not modified significantly by mixing with PEG (the shifts are within the spectral resolution). Although the $\nu(C_\beta{-}C_\gamma)$ band remains stronger in all the spectra, in the studied nicotine solutions its relative intensity decreases, slightly more in the case of PEG200. This may be due to van der Waals interactions with the polymer, but the modifications are significantly weaker than those observed for pyridine in the pyridine + PEG200/400 solutions.

Comparison between Pyridine + PEG200/400 and Nicotine + PEG200/PEG400 Solutions. The above spectral analysis shows that pyridine and PEG strongly interfere with each other. On the contrary, the geometry of the nicotine molecule is hardly affected by the presence of the liquid polymer; the methylpyrrolidine ring remains nonplanar as in pure nicotine.[7−9] This represents a significant steric hindrance to the approach of the PEG chains to establish the very directional hydrogen bonds with the nitrogen lone pairs of the pyridine ring. Hence, much weaker intermolecular hydrogen bonds and, consequently, much less negative molar excess volumes are expected in the nicotine solutions ; see Figures 5 and 6. Furthermore, this is a dominant effect that reduces the impact of the PEG chain length on the results for the nicotine solutions with respect to that observed in the pyridine solutions. Thus, the striking differences between the minimum values of V^E observed in Figures 7 and 8 may be better understood.

The temperature effect on the V^E of the nicotine systems is also consistent with the proposed interactions. Hydrogen bonds

are much weaker in the studied nicotine solutions, but dispersion interactions are more important since the polarizability of nicotine is much higher. The latter interactions decrease substantially as the temperature increases.[36] The conformational rearrangements in pyridine + PEG200/400 solutions are not present in the case of nicotine, as evidenced by the spectra, which is consistent with the results obtained for V^E.

CONCLUSIONS

The experimental molar excess volumes of the pyridine/nicotine + PEG200/PEG400 solutions revealed negative values for all the studied systems, thus clearly indicating strong attractive interactions between the components—hydrogen bonds and dipole−dipole interactions: Keesom and dispersive forces. This is reasonable to expect, taking into consideration good hydrogen-bonding abilities and high dipole moments and polarizabilities of the constituents. For the pyridine solutions, the molar excess volumes become more negative as the temperature increases, while the opposite effect occurs for solutions with nicotine. This difference in the V^E temperature dependence between the pyridine and nicotine solutions may mainly be interpreted by the distinct isobaric thermal expansion coefficients and critical temperatures of the pure components of the two types of systems.

Pyridine solutions exhibited much more negative molar excess volumes than those of nicotine. However, though neat PEG200 has higher hydrogen bond acidity than PEG400, the latter provoked more negative molar excess volumes than PEG200 when mixed with pyridine. Moreover, a high impact of the polymer chain length on negative molar excess volumes—inducing significantly higher negativity—is present in pyridine solutions, whereas it is quite negligible in nicotine solutions.

FTIR analysis enlightened the possible causes for the aforementioned behaviors. The obtained spectra showed the following: (i) The hydrogen bonds in pyridine solutions with PEG400 are stronger than in those with PEG200. (ii) The conformational diversity in pure PEG400—almost absent in PEG200—generally facilitates its ability to establish hydrogen bonding. (iii) Intermolecular hydrogen bonds in the nicotine solutions have much lower intensity than those in pyridine. (iv) In the pyridine solutions, especially in those with PEG400, the strong attractive interactions affect the molecules of both constituents: the presence of pyridine shifts the PEG conformational distribution toward the *gauche*, and the interactions with the polymer deform the pyridine molecule, thus reducing its symmetry. (v) For the nicotine solutions a much smaller mutual influence of the two unlike molecules is observed, which is to be expected since the interactions themselves are of much lower intensity.

The effect of steric factors on the results is present as well. Nicotine has a spatial configuration that is not suitable for dense packing and obstructs strong, oriented interactions with the large PEG molecules. The latter claim is supported by the spectral results; the shifts of the OH stretching mode of the liquid polymers related to the hydrogen bonds with pyridine or nicotine are much lower in the case of nicotine solutions. In contrast, pyridine is smaller and deforms in the presence of PEG.

ASSOCIATED CONTENT

Supporting Information. Deconvolutions of the FTIR spectra of the studied solutions and of the respective pure components, tables with the parameters of the Voigt components obtained by spectral deconvolution, and a table with the densities and molar excess volumes of all the systems at every studied isotherm. This material is available free of charge via the Internet at http://pubs.acs.org.

AUTHOR INFORMATION

Corresponding Author

*E-mail: zoran.visak@ist.utl.pt. Phone: ++351-21-841-9229. Fax: ++351-21-846-4455.

ACKNOWLEDGMENT

The Serbian authors gratefully acknowledge the financial support received from the Research Fund of the Ministry of Science and Environmental Protection, Serbia, and the Faculty of Technology and Metallurgy, University of Belgrade (Project 172063).

REFERENCES

(1) Sherman, A. R. *Encyclopedia of Reagents for Organic Synthesis: Pyridine*; J. Wiley & Sons: Hoboken, NJ, 2004.
(2) Shimohama, S. *Biol. Pharm. Bull.* **2009**, *32*, 332–336.
(3) Dipti, M.; Rastogi, P. P. *Bull. Chem. Soc. Jpn.* **1976**, *49*, 206–208.
(4) Ochoa, M. L.; Harrington, P. B. *Anal. Chem.* **2004**, *76*, 985–991.
(5) Abraham, M. H.; Grellier, P. L.; Prior, D. V.; Morris, J. J.; Taylor, P. J. *J. Chem. Soc., Perkin Trans. 2* **1990**, 521–529.
(6) Graton, J.; Berthelot, M.; Gal., J.-F.; Girard, S.; Laurence, C.; Lebreton, J.; Le Questel, J. -Y.; Maria, P.-C.; Nauš, P. *J. Am. Chem. Soc.* **2002**, *124*, 10552–10562.
(7) Elmore, D. E.; Dougherty, D. A. *J. Org. Chem.* **2000**, *65*, 742–747.
(8) Whidby, J. F.; Edwards, W. B., III; Pitner, T. P. *J. Org. Chem.* **1979**, *44*, 794–798.
(9) Pitner, T. P.; Edwards, W. B., III; Bassfield, R. L.; Whidby, J. F. *J. Am. Chem. Soc.* **1978**, 246–251.
(10) Heldebrant, D. J.; Witt, H. N.; Walsh, S. M.; Ellis, T.; Rauscher, J.; Jessop, P. G. *Green Chem.* **2006**, *8*, 807–815.
(11) Sengwa, R. J.; Kaur, K.; Chaudhary, R. *Polym. Int.* **2000**, *49*, 599–608.
(12) Rudan-Tasic, D.; Klofutar, C. *Monatsh. Chem.* **2005**, *136*, 1171–1182.
(13) Kim, I.-W.; Jang, M. D.; Ryu, Y. K.; Cho, E. H.; Lee, Y. K.; Park, J. H. *Anal. Sci.* **2002**, *18*, 1357–1360.
(14) Donaldson, M. E.; Draucker, L. C.; Blasucci, V.; Liotta, C. L.; Eckert, C. A. *Fluid Phase Equilib.* **2009**, *277*, 81–86.
(15) Liang, J.; Jing, Lv.; Fan, J.; Shang, Z. *Synth. Commun.* **2009**, *39*, 2822–2828.
(16) Chen, C.; Even, M. A.; Wang, J.; Chen, Z. *Macromolecules* **2002**, *35*, 9130–9135.
(17) Long, D. A.; Murfin, F. S.; Thomas, E. L. *Trans. Faraday Soc.* **1963**, *59*, 12–24.
(18) Perelygin, I. S.; Klimchuk, M. A. *Zh. Prikl. Spektrosk.* **1976**, *24*, 65–68.
(19) Ureña, F. P.; Gómez, M. F.; González, J. J. L.; Torres, E. M. *Spectrochim. Acta, A* **2003**, *59*, 2815–2839.
(20) Unger, E.; Lipski, R. J.; Dreybrodt, W.; Schweitzer-Stenner, R. *J. Raman Spectrosc.* **1999**, *30*, 3–28.
(21) El-Gogary, T. M.; Soliman, M. S. *Spectrochim. Acta, A* **2001**, *57*, 2647–2657.
(22) Eddy, C. R.; Eisner, A. *Anal. Chem.* **1954**, *26*, 1428–1431.
(23) Garrigues, J. M.; Pérez-Ponce, A.; Garrigues, S.; de la Guardia, M. *Anal. Chim. Acta* **1998**, *373*, 63–71.
(24) Ottani, S.; Vitalini, D.; Comelli, F.; Castellari, C. *J. Chem. Eng. Data* **2002**, *47*, 1197–1204.

(25) Mūller, E. A.; Rasmussen, P. *J. Chem. Eng. Data* **1991**, *36*, 214–217.
(26) Han, F.; Zhang, J.; Chen, G.; Wei, X. *J. Chem. Eng. Data* **2008**, *53*, 2598–2601.
(27) Eliassi, A.; Modarress, H. *J. Chem. Eng. Data* **1998**, *43*, 719–721.
(28) Helm, R. V.; Lanum, W. J.; Cook, G. L.; Ball, J. S. *J. Phys. Chem.* **1958**, *62*, 858–862.
(29) Campbell, A. N.; Kartzmark, E. M.; Falconer, W. E. *Can. J. Chem.* **1958**, *36*, 1475–1486.
(30) Chirico, R. D.; Steele, W. V.; Nguyen, A.; Klots, T. D.; Knipmeyer, S. E. *J. Chem. Thermodyn.* **1996**, *28*, 797–818.
(31) Manic, M. S.; Najdanovic-Visak, V.; Nunes da Ponte, M.; Visak, Z. P. *AIChE J.* **2010**, *54*, 1344–1355.
(32) Rozenberg, M.; Loewenschuss, A.; Marcus, Y. *Spectrochim. Acta, A* **1998**, *54*, 1819–1826.
(33) Harder, P.; Grunze, M.; Dahint, R.; Whitesides, G. M.; Laibinis, P. E. *J. Phys. Chem. B* **1998**, *102*, 426–436.
(34) Öztürk, N.; Ucun, F.; Muhtar, A. D.; Bahçeli, S. *J. Mol. Struct.* **2009**, *922*, 35–38.
(35) Dougherty, R. C. *J. Chem. Phys.* **1998**, *109*, 7372–7378.
(36) Israelachvili, J. *Intermolecular & Surface Forces*, 2nd ed.; Academic: New York, 1992.